The polarised gluon density from di-jet events in DIS at a polarised HERA

G. Rädel[a], A. De Roeck[b], M. Maul[c]

[a] *CERN - Div. PPE, 1211 Genève 23, Switzerland.*

[b] *DESY - FH1, Notkestr. 85, 22603 Hamburg, Germany*

[c] *Institut für Theoretische Physik der Universität Regensburg, 93040 Regensburg, Germany*

Abstract

We present a possible direct measurement of the polarised gluon density $\Delta G(x)$ in LO from di-jet production in polarised deep inelastic ep scattering, assuming the kinematics of the HERA collider. We show the sensitivity to the x-dependence of $\Delta G(x)$ and to the first moment $\int \Delta G(x)dx$ in the range $0.002 < x < 0.2$, assuming the electron and proton beam of HERA being polarised to 70% and an integrated luminosity of at least 200 pb^{-1}. We include in our study hadronisation and higher order effects, as well as realistic detector smearing and acceptance. We find that the statistical and systematic uncertainties are small enough to distinguish between different parametrizations for $\Delta G(x)$, which all are in accordance with present data. We stress that at HERA an x-range could be measured, that is not accessible to any other present or proposed experiment.

1 Introduction

The precise study of the nucleon spin structure has evolved over the last years into a broad field allowing to test many aspects of QCD. The surprising EMC [1] result, that the quarks carry only a small fraction of the nucleon spin, has been confirmed by new high precision measurements. This dramatic improvement in quality of the data and theoretical analysis has lead to a generally accepted range of polarised parton distribution parametrizations which imply that the quarks carry only about 30% of the nucleon spin. Nearly all models predict a substantial polarisation for both the gluons and the strange quarks which has to be confirmed by direct experimental tests before the present standard interpretation of the data can be regarded as established. The polarised gluon distribution is of special interest since it could be surprisingly large.

In the next to leading order (NLO) evolution equations the quark and gluon distributions mix, hence polarised gluons also contribute to $g_1(x, Q^2)$. The quality of the present g_1 data allow for QCD fits to be made, and ΔG to be extracted. The precision is however rather poor, and only some information on the first moment on ΔG is obtained. Therefore the hunting of ΔG by direct measurements is one of the key issues in polarised scattering physics for the next foreseeable future.

The unpolarised gluon distribution has been studied at the ep collider HERA. The large centre of mass energy ($\sqrt{s} = 300$) GeV, resulting from 27.5 GeV electrons colliding with 820

GeV protons, allows for several techniques to be used. So far the gluon distribution at HERA has been accessed via scaling violations of F_2, di-jet production, charm production and exclusive vector meson production. While the first method gives an indirect measurement of the gluon, like for the NLO analysis of g_1, for the other methods the gluon enters directly at the Born level. In this paper we will use the method of extracting the gluon via di-jet events rates.

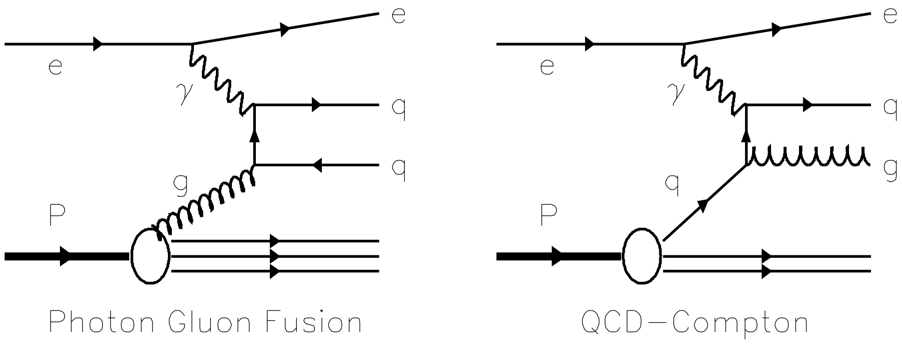

Figure 1: Feynman diagrams for the di-jet cross sections at LO, the Photon-Gluon Fusion (PGF) process (left) and the QCD-Compton process (right).

In LO two diagrams can lead to di-jet events, shown in Fig. 1. These are the Photon-Gluon Fusion process (PGF) and the QCD-Compton process (QCDC). The PGF process is directly sensitive to the gluon density, while the QCDC process is sensitive to the quark densities and constitutes the background. The H1 collaboration has performed an analysis of di-jets to extract the PGF contribution and thus the gluon distribution [2]. Presently both the H1 an ZEUS collaborations attempt to extract the gluon distribution at NLO from di-jets event rates [3, 4].

If both beams at HERA would be polarised, this method could be used to extract ΔG. Due to the Sokolov-Ternov effect the electron beam gets transversely polarised in the machine. Spin rotators can flip transverse into longitudinal polarisation, which is more useful for physics studies. The only possibility for a polarised proton beam at HERA is to start from a polarised source and accelerate and store the beam, keeping the polarisation on the way [5]. First feasibility studies indicate the possibility of such a scenario in case the accelerators get upgraded with partial and full Siberian snakes. For this report it is assumed that a polarisation of 70% can be reached for both beams, and that the luminosity will be as large as for the unpolarised case (roughly 200 to 500 pb^{-1}, integrated over several years)

First studies on extracting ΔG from di-jet event rates were made in [6, 7]. In this paper we make a full Monte Carlo simulation of the signal and background processes, include hadronisation, higher order effects via parton showers, and detector effects. Starting from three different sets of polarised gluon distributions, shown in Fig. 2, we check the sensitivity of the measurements and extract $\Delta G(x)$. These distributions are the Gehrmann-Stirling (GS) sets A and C [8], which result from a QCD analysis of g_1 data, and the instanton-gluon distribution [9]. The latter results from a calculation of the polarised parton distribution in the Instanton Liquid Model [10]. The distributions shown in Fig. 2, purposely selected, indicate how poorly $\Delta G(x)$ is constrained

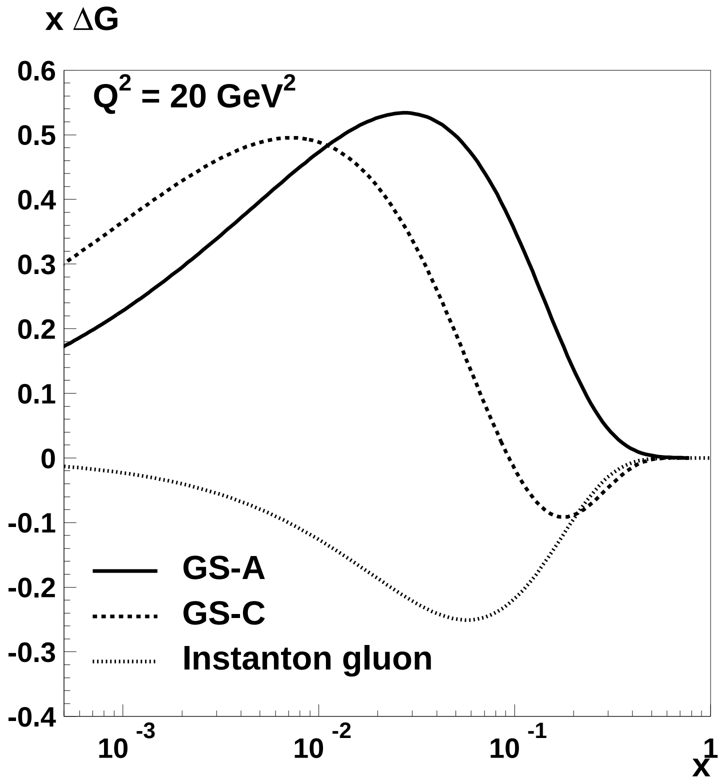

Figure 2: Different parametrizations of the polarised gluon density as a function of x used in this analysis, described in the text.

by the present polarised data. All of these distributions are compatible with the available data, stressing the need for direct measurements of $\Delta G(x)$. The GS-A and GS-C distribution show a similar small x behaviour, but differ considerably in the region around $x \sim 0.1$. The GS-C distribution is negative for this x region. The instanton-gluon is quite different from the GS sets. It remains negative over the full x range. The latter gluon is used in combination with the GS-A quark distributions for the study in this paper. For the unpolarised parton density functions the parametrizations of Glück, Reya and Vogt in LO were used [11].

2 Jet cross sections and Monte Carlo programs

Deep inelastic electron-proton scattering with several partons in the final state,

$$e^-(l) + p(P) \to e^-(l') + \text{remnant}(p_r) + \text{parton } 1(p_1) + \ldots + \text{parton } n(p_n) \qquad (1)$$

proceeds via the exchange of an intermediate vector boson $V = \gamma^*, Z$. Z-exchange and γ^*/Z interference become only important at large Q^2 (> 1000 GeV^2) and are neglected in the following. We denote the momentum of the incoming proton by P, the momentum of the virtual photon, γ^*, by $q = l - l'$, (minus) its absolute square by Q^2, and use the standard scaling variables Bjorken-x $x = Q^2/(2P\cdot q)$ and inelasticity $y = P\cdot q/P\cdot l$. The general structure of the unpolarised n-jet cross section in DIS is given by

$$d\sigma^{had}[n\text{-jet}] = \sum_a \int dx_a \; f_a(x_a, \mu_F^2) \;\; d\hat{\sigma}^a(p = x_a P, \alpha_s(\mu_R^2), \mu_R^2, \mu_F^2) \qquad (2)$$

where the sum runs over incident partons $a = q, \bar{q}, g$ which carry a fraction x_a of the proton momentum. $\hat{\sigma}^a$ denotes the partonic cross section from which collinear initial state singularities have been factorized out (in next-to-leading order (NLO)) at a scale μ_F and implicitly included in the scale dependent parton densities $f_a(x_a, \mu_F^2)$. For longitudinally polarised lepton-hadron scattering, the hadronic (n-jet) cross section is obtained from Eq. (2) by replacing $(\sigma^{had}, f_a\ , \hat{\sigma}^a) \rightarrow (\Delta\sigma^{had}, \Delta f_a, \Delta\hat{\sigma}^a)$. The polarised hadronic cross section is defined by $\Delta\sigma^{had} \equiv \sigma^{had}_{\uparrow\downarrow} - \sigma^{had}_{\uparrow\uparrow}$, where the left arrow in the subscript denotes the polarisation of the incoming lepton with respect to the direction of its momentum. The right arrow stands for the polarisation of the proton parallel or anti-parallel to the polarisation of the incoming lepton. The polarised parton distributions are defined by $\Delta f_a(x_a, \mu_F^2) \equiv f_{a\uparrow}(x_a, \mu_F^2) - f_{a\downarrow}(x_a, \mu_F^2)$. Here, $f_{a\uparrow}(f_{a\downarrow})$ denotes the probability to find a parton a in the longitudinally polarised proton whose spin is aligned (anti-aligned) to the proton's spin. $\Delta\hat{\sigma}^a$ is the corresponding polarised partonic cross section. The subprocesses $\gamma^* + q \rightarrow q + g$, $\gamma^* + \bar{q} \rightarrow \bar{q} + g$, $\gamma^* + g \rightarrow q + \bar{q}$ contribute to the di-jet cross section (Fig. 1). The photon-gluon fusion subprocess $\gamma^* + g \rightarrow q + \bar{q}$ dominates the di-jet cross section at low Bjorken-x for unpolarised protons (see below) and allows for a direct measurement of the gluon density in the proton. The full NLO corrections for di-jet production in unpolarised lepton-hadron scattering are implemented in the $ep \rightarrow n -$ jets event generator MEPJET [12] which allows to analyse arbitrary jet definition schemes and general cuts in terms of parton 4-momenta. Recently, MEPJET has been extended to NLO for polarised scattering [13], and the NLO QCD corrections are found to be moderate.
In LO the total unpolarised di-jet cross section is the sum of the contributions from photon gluon fusion processes, $\sigma^{PGF}_{di\text{-}jet}$, and QCD-Compton scattering, $\sigma^{QCDC}_{di\text{-}jet}$ and can be written as:

$$\sigma_{di\text{-}jet} = \sigma^{PGF}_{di\text{-}jet} + \sigma^{QCDC}_{di\text{-}jet} = A\ G + B\ q \tag{3}$$

where G and q are the gluon and quark densities and A and B can be calculated in perturbative QCD. Similarly, for the polarised case we can write:

$$\Delta\sigma_{di\text{-}jet} = \sigma^{\uparrow\downarrow}_{di\text{-}jet} - \sigma^{\uparrow\uparrow}_{di\text{-}jet} = a\ \Delta G + b\ \Delta q \tag{4}$$

with ΔG and Δq being the polarised gluon and quark densities. The di-jet asymmetry is therefore sensitive to $\Delta G/G$, especially at low x where the PGF cross section dominates.

$$A_{di\text{-}jet} = \frac{\Delta\sigma_{di\text{-}jet}}{2\,\sigma_{di\text{-}jet}} = \mathcal{A}\ \frac{\Delta G}{G}\ \frac{\sigma^{PGF}_{di\text{-}jet}}{2\,\sigma_{di\text{-}jet}} + \mathcal{B}\ \frac{\Delta q}{q}\ \frac{1}{2}(1 - \frac{\sigma^{PGF}_{di\text{-}jet}}{\sigma_{di\text{-}jet}}), \tag{5}$$

with $\mathcal{A} \equiv a/A$ and $\mathcal{B} \equiv b/B$. The experimentally accessible asymmetry A_{meas} is smaller than $A_{di\text{-}jet}$ due to the incomplete polarisations of the electron and proton beams, given by P_e, P_p, and the depolarisation of the γ^* with respect to the electron. The latter effect is described by the depolarisation factor $D = (y(2-y))/(y^2 + 2(1-y)(1+R))$, where y is the inelasticity and R is the ratio of longitudinal and transverse $\gamma^* p$ cross sections.

$$A_{meas} = \frac{N^{\uparrow\downarrow} - N^{\uparrow\uparrow}}{N^{\uparrow\downarrow} + N^{\uparrow\uparrow}} = P_e P_p D A_{di\text{-}jet} \tag{6}$$

The quantities $N^{\uparrow\downarrow}$ ($N^{\uparrow\uparrow}$) are the total number of observed di-jet events ($N^{\uparrow\downarrow} = N^{\uparrow\downarrow}_{PGF} + N^{\uparrow\downarrow}_{QCDC}$) for the case that proton and electron spin are antiparallel (parallel), respectively. The kinematic quantities to describe the PGF process are the momentum fraction of the proton carried by the gluon x_g, the four-momentum transfer Q^2 and the square of the invariant mass of the two jets s_{ij}. They are related to the Bjorken-x, x, by:

$$x_g = x(1 + \frac{s_{ij}}{Q^2}).$$

For $s_{ij} > 100$ GeV^2, and in the Q^2 range relevant for HERA of $5 < Q^2 < 100$ GeV^2, x_g is larger than Bjorken-x by about an order of magnitude and the accessible range at HERA is therefore about $0.002 < x_g < 0.2$. H1 has demonstrated that in this region the unpolarised gluon density $G(x)$ can be extracted from di-jet cross sections [2].

The program MEPJET has been used to study di-jet production in (un)polarised DIS at (N)LO at the level of parton-jets [6, 7, 12]. To perform a study for a possible future measurement it is, however, desirable to include also hadronisation and detector effects. Therefore in this study we use the Monte Carlo event generator program PEPSI 6.5 [14, 15]. It is a full, LO lepton-nucleon scattering Monte Carlo program based on LEPTO 6.5 [16] for unpolarised and polarised interactions, including fragmentation, and unpolarised parton showers to simulate higher order effects.

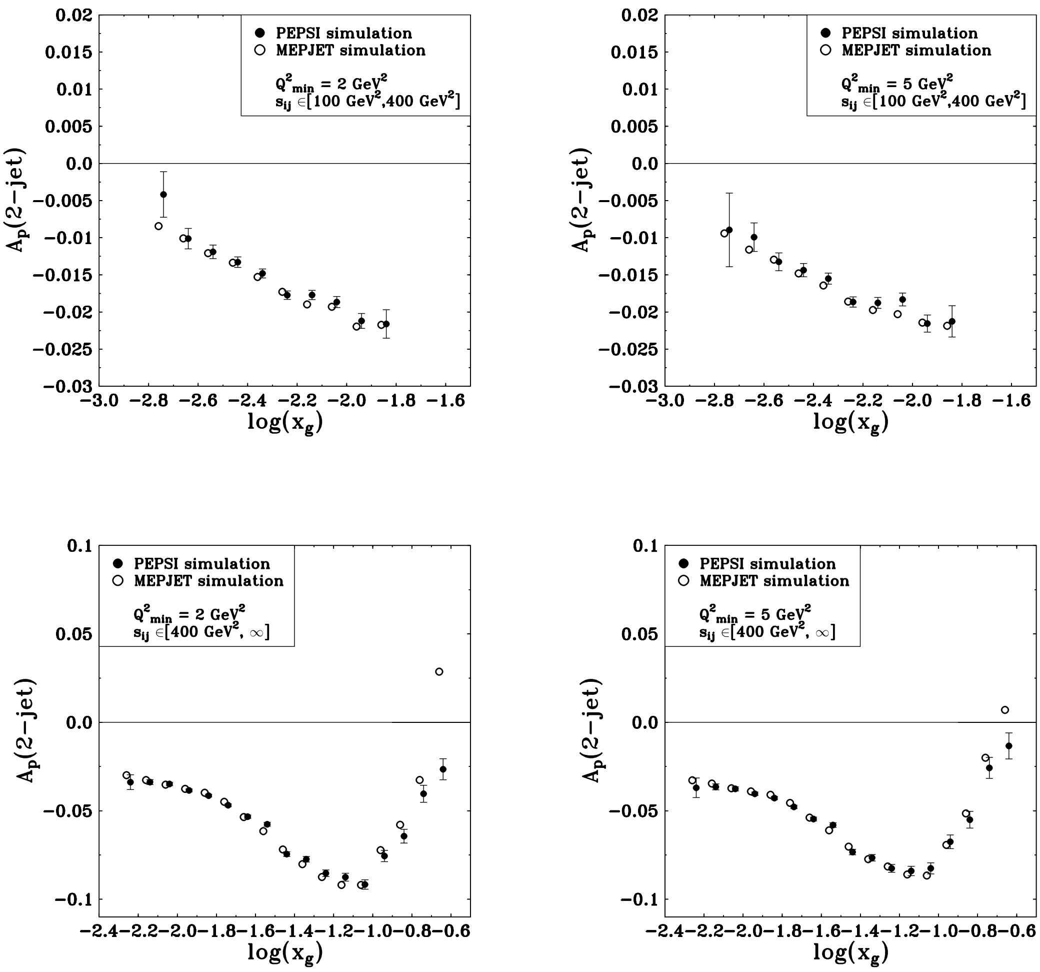

Figure 3: Comparison of the di-jet cross sections obtained with the MC programs MEPJET and PEPSI 6.5. The cross sections are shown for different bins of s_{ij} and for a lower Q^2-cut of 2 and 5 GeV^2. The error bars for the PEPSI study represent the statistical uncertainty corresponding to the generated number of events.

A comparison of PEPSI and MEPJET, used with identical conditions and cuts, shows that, at parton level, both programs give very similar results for di-jet cross sections and asymmetries for the HERA kinematic range [17]. As an example Fig. 3 shows the comparison for the di-jet asymmetry (A_p(2-jets) $\equiv D\, A_{di\text{-}jet}$) as function of x_g. The agreement between the MEPJET and PEPSI calculation is very good. The calculations were done for HERA energies, 820 GeV protons and 27.5 GeV electrons. The kinematic range was restricted to $0.3 < y < 0.8$ and $Q^2 < 100$ GeV^2. The minimum Q^2 was varied from 2 GeV^2 (plots on the left) to 5 GeV^2 (plots on the right). In PEPSI the so-called z-$\hat{s}$ recombination scheme [18] has been used to define the phase space available for the LO matrix elements. The parameters for this scheme, $z_{min} = 0.04$ and $\hat{s}_{min} = 100$ GeV^2, were chosen such that the phase space region for di-jet events using a cone jet scheme for di-jets with $p_t > 5$ GeV and $s_{ij} > 100$ GeV^2 was not affected. z_{min} is the minimum of $z = (P \cdot p_{jet})/(P \cdot q)$ for the two jet momenta p_{jet} in a di-jet event. The variable $\hat{s}$ is defined via $\hat{s} \equiv (p+q)^2$, where p is the momentum of the incoming quark. For the jet detection a cone jet algorithm was used with $R_{min} = 1$, R_{min} being the minimal distance which two partons must have in order to belong to different jets. R is given by: $R = \sqrt{(\Delta\eta)^2 + (\Delta\phi)^2}$ with η being the pseudo rapidity and ϕ being the azimuthal angle in the laboratory frame. The two upper plots show the asymmetries for events with $100 < s_{ij} < 400$ GeV^2, for the two lower plots $s_{ij} > 400$ GeV^2. The division into two s_{ij} bins was made, because studies for the unpolarised di-jet cross sections [12, 6] have shown that NLO corrections are expected to be small above $s_{ij} \gtrsim 400$ GeV^2.

In ref. [17] a study was made to further optimize the cuts in order to get a better sensitivity to ΔG. They concluded that the cuts used in this analysis are already very close to the optimum choice.

Recently, some disagreement at low Q^2 has been reported between the newly, more precise, measured jet cross sections and the NLO calculations at HERA, using the cone jet algorithm [19]. This discrepancy may hint towards a 'resolved' photon component in the data, and is presently under study. We expect however that at the time the measurement described in this paper can be made, this matter will be settled and will have the effect of an additional small background to be subtracted from the di-jet event rates, in order to access the gluon distribution.

3 Measured asymmetries

We present a detailed study using the PEPSI program on the expected size of the measurable asymmetries for di-jet production at HERA. We show the influence of parton showers, which simulate higher order effects, and hadronisation and detector effects. We also show the sensitivity of the measurement to different polarised gluon distributions.

The kinematic cuts applied for this study are similar to the ones discussed in the previous section, $5 < Q^2 < 100$ GeV^2 and $0.3 < y < 0.85$. Again two bins of s_{ij} were analysed with $100 < s_{ij} < 400$ GeV^2 and $s_{ij} > 400$ GeV^2, respectively. Jets are defined using the cone scheme, are required to have a $p_t > 5$ GeV and are restricted to the acceptance of a typical existing HERA detector by $|\eta_{jet}| < 2.8$, were η_{jet} is the pseudo-rapidity in the laboratory system. The expected measurable asymmetry for the input polarised gluon density GS-A, assuming the beam polarisations $P_e = P_p = 0.7$ and 200 pb^{-1} for the luminosity, is shown in Fig. 4a at the parton level. The expected asymmetry is negative and of the order of a few %. Jets induced by parton showers tend to reduce the size of the asymmetry. This is due to the fact that parton showers can produce a hard jet, which is then misidentified as a PGF induced one. This, rather small reduction on parton level, is more pronounced, if hadronisation and detector smearing effects are included (see Fig. 4b). The reason for this is that both effects broaden the jets and therefore the measured p_t which is related to the energy in the cone of fixed size is smaller than the p_t of the parton jet. The reconstruction of the kinematics of the event (s_{ij}, x_g) is influenced and the correlation with the parton jets is reduced. For the hadronisation the Lund fragmentation model, implemented in JETSET [20], was used and an energy resolution for the hadronic calorimeter of $\Delta E_{had}/E_{had} = 0.5/\sqrt{E_{had}[\mathrm{GeV}]}$ was assumed. The results were cross checked using a realistic

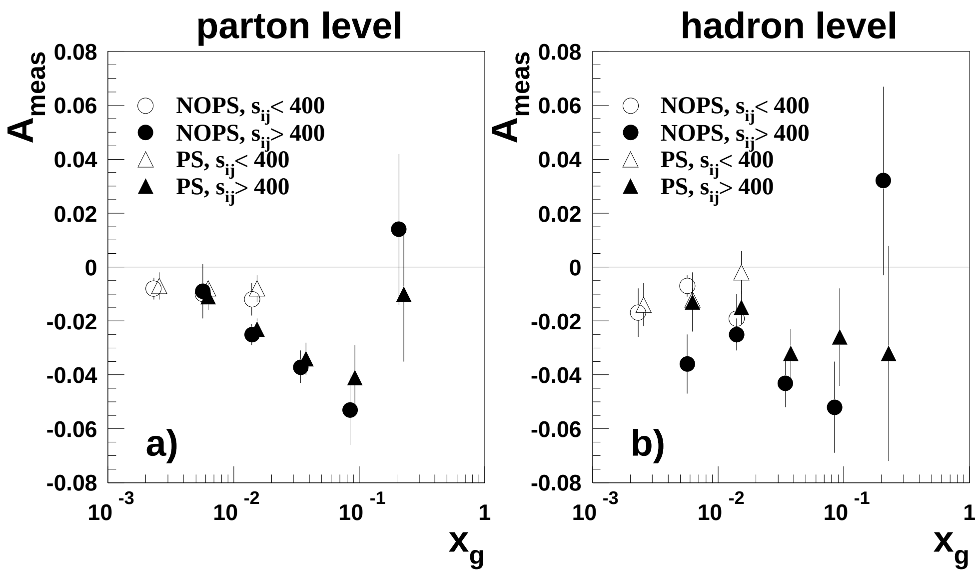

Figure 4: Expected measured asymmetries for di-jet events as a function of x_g calculated with PEPSI on the parton level (a) and detector level (b). For each case the asymmetries are shown with (PS) and without (NOPS) parton showers for two different ranges of s_{ij}. The assumed integrated luminosity is 200 pb^{-1}. The input polarised gluon distribution is GS-A.

simulation program of the H1 calorimeter [21], which takes into account the energy resolution, the absolute energy scale and dead material in the detector. In order to optimize the signal to background ratio cuts were introduced demanding the two jets to be produced with a restricted difference in pseudo-rapidity and back to back in azimuth, as it is expected for real PGF events: $|\eta_{jet1} - \eta_{jet2}| < 2$ and $150° < \phi_{jet1} - \phi_{jet2} < 210°$. After all these cuts for 100 pb^{-1} about 70,000 di-jet events are selected. The ratio of QCDC - PGF events is in the order of 1:6. The average Q^2 of this event sample is very close to 20 GeV^2 therefore results for ΔG are presented at this value.

All cuts are applied in the asymmetry shown in Fig. 4b. Although the asymmetries are smaller due to the parton showers, and the statistics is reduced compared to the result on parton level, the expected asymmetry is still large enough to allow a statistically significant measurement for 200 pb^{-1}. These asymmetries form the basis of the studies in this paper. Due to the split-up in the s_{ij}-bins, for the second and third x_g bin there are two measurements. For simplicity we choose in the following one measurement per x_g-bin, i.e. the one with the better significance. However, in principal the other points could be used as well, and add to the statistical significance. Table 1

x_g	$5 < Q^2 < 100$ GeV^2 A_{meas}	A_{corr}	$\delta(A)$
0.002	-0.016	-0.016	0.008
0.006	-0.012	-0.012	0.004
0.014	-0.015	-0.018	0.005
0.034	-0.032	-0.032	0.009
0.084	-0.026	-0.047	0.018
0.207	-0.032	-0.069	0.040

x_g	$2 < Q^2 < 10$ GeV^2 A_{corr}	$\delta(A)$	$10 < Q^2 < 100$ GeV^2 A_{corr}	$\delta(A)$
0.002	-0.009	0.009	-0.006	0.010
0.006	-0.010	0.005	-0.014	0.005
0.014	-0.017	0.007	-0.026	0.007
0.034	-0.042	0.010	-0.037	0.010
0.084	-0.045	0.021	-0.073	0.021
0.207	-0.096	0.046	-0.008	0.050

Table 1: Expected measured asymmetries from di-jet events at HERA and background corrected asymmetries with statistical errors corresponding to an integrated luminosity of 200 pb^{-1}. The right table shows the background corrected asymmetries for two different Q^2 ranges.

shows the expected asymmetries A_{meas} and their statistical errors $\delta(A)$ for the six x_g-bins shown in Fig. 4. The two lowest x_g-bins correspond to $100 < s_{ij} < 400$ GeV^2. Also shown is A_{corr} which is defined as $A_{corr} = \frac{N_{PGF}^{\uparrow\downarrow} - N_{PGF}^{\uparrow\uparrow}}{N^{\uparrow\downarrow} + N^{\uparrow\uparrow}}$ and corresponds to the first term in the sum of Eq. 5, which is the part sensitive to $\Delta G/G$. In other words, it is the measured asymmetry corrected for the QCDC contribution. The numbers in Table 1 show that a significant contribution from QCDC processes is expected only for the two highest x_g-bins.

The right part of Table 1 shows results for A_{corr} and its statistical error if the low Q^2 cut is released to 2 GeV^2 and the data are divided into to Q^2 bins. The mean Q^2 values for the two bins are 4.5 GeV^2 and 30 GeV^2, respectively.

Fig. 5 shows the expected measurable asymmetries for different sets of polarised gluon densities, i.e. the ones shown in Fig. 2: GS-A, GS-C, and the instanton-gluon. For the latter the polarised quark densities were taken from [8]. The assumed luminosity is 200 pb^{-1}. It can be seen here that the measurable asymmetry is very sensitive to the gluon input. The negative instanton-ΔG leads to a positive asymmetry and can be clearly distinguished from the other two sets. GS-A and GS-C can be discriminated in the higher x-range, which is where they are maximally different.

4 Extraction of ΔG

In this section we will quantify the sensitivity to the shape of $\Delta G/G$ and discuss systematic uncertainties. In a real measurement one could obtain $\Delta G/G$ from the measured asymmetry by an unfolding method, where the background would be subtracted statistically and correlations between bins are fully taken into account. Such a method was used by H1 to extract the unpolarised gluon density [2]. If correlations between bins are small one can use a simpler method performing a bin-by-bin correction. For our study we consider the latter method to be sufficient.

We simulate 500 pb^{-1} of di-jet events, as described in Sect. 3 with GS-A as input gluon density. This would in a real measurement correspond to the Monte Carlo generation of events and will therefore be called 'MC-set' here. Assuming that for each x-bin $\Delta G/G$ and A_{corr} are

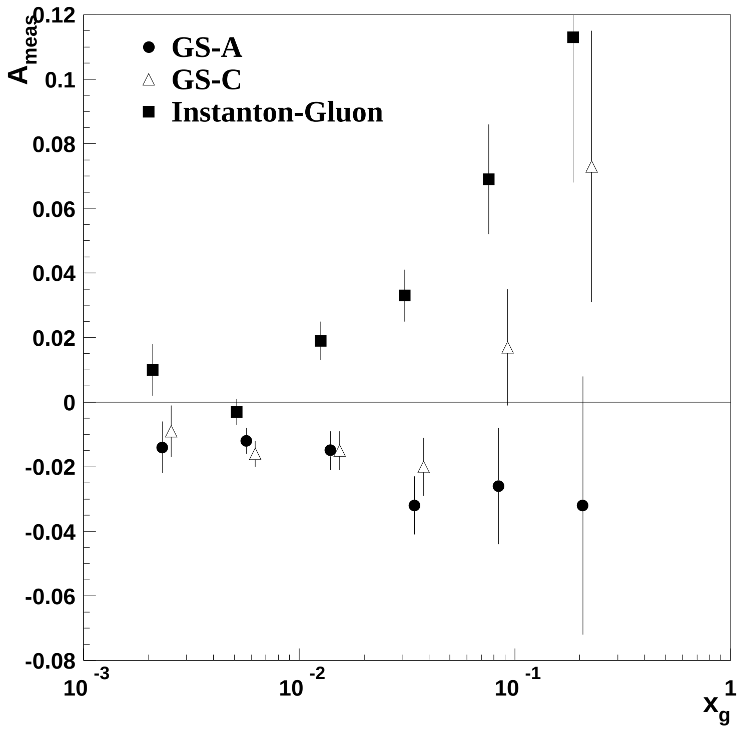

Figure 5: Expected measured asymmetries for di-jet events for different input polarised gluon densities. The assumed integrated luminosity is 200 pb^{-1}.

related to each other by a simple factor F_i:

$$\left(\frac{\Delta G}{G}\right)_i = F_i \cdot A_{corr,\,i},$$

where i indicates the x-bin, we compute these factors using the MC-set.

These factors F_i were then multiplied with the asymmetries A_{corr} that correspond to the three measured asymmetries in Fig. 5. The three sets of events used here represent the possible measurements and are called 'data sets'. The result is shown in Figs. 6a - 6c. Within the statistical accuracy the input (solid lines) $\Delta G/G$ is found back for all cases and the statistics is sufficient to discriminate between them. The six x-points allow in particular a measurement of the shape of the polarised gluon distribution. (The statistical fluctuations for GS-A are smaller than can be expected because the data set of 200 pb^{-1} which was used to produce the asymmetry was also included in the MC-set used to determine the correction factors F_i.) The errors shown reflect the statistics of the data sets (200 pb^{-1}). The statistical uncertainty of the F_i is not included here, since in a real measurement it would be computed with very high statistical precision. However, the limited statistics here is reflected in the fluctuations in Fig. 6. Figures 6d - 6f shows the same result presented for the theoretically more interesting quantity $x\Delta G$. The error bars are scaled errors of the left column, i. e. no uncertainty was assigned to G at this stage.

After we have shown that the measurable asymmetries are sensitive to the input of ΔG and that we are able to extract the polarised gluon densities in several x-bins, the sensitivity to the shape of $\Delta G/G$ and $x\Delta G$ for an integrated luminosity of 500 pb^{-1} is shown in Fig. 7. The

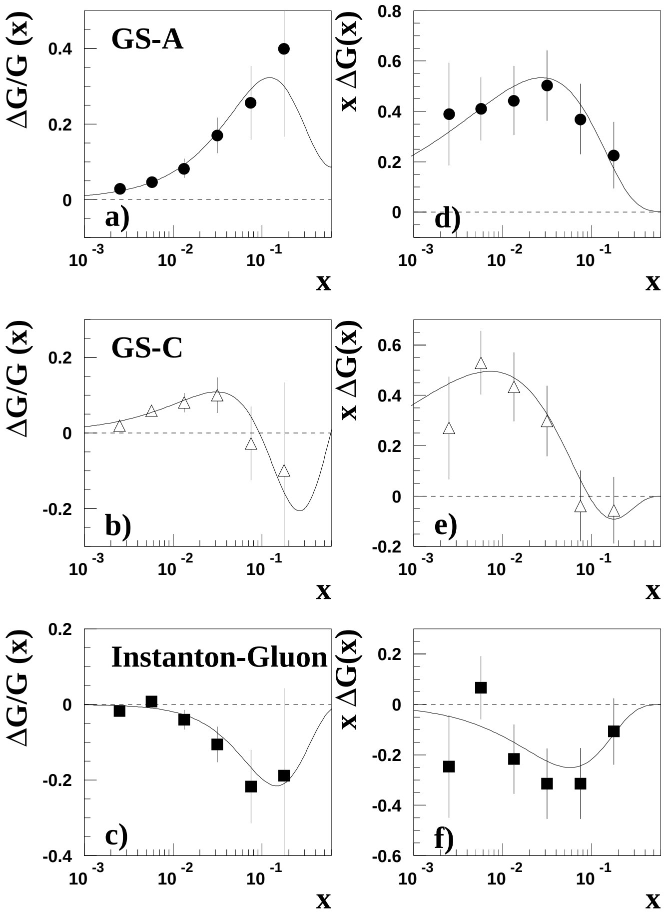

Figure 6: For a luminosity of 200 pb^{-1} the sensitivity to extract $\Delta G/G$ (a-c) and $x\Delta G$ (d-f) is shown for different polarised gluon densities (see text).

statistical errors for the x points are shown on the curves for $\Delta G/G$ (a-c) and $x\Delta G$ (d-f). Again we notice the good separation between the different distributions. A study was performed on the systematic errors for the GS-A polarised gluon distribution. The error sources considered were: an uncertainty of 2% of the calibration of the hadronic energy scale, an error on the total unpolarised di-jet cross section $\sigma_{di\text{-}jet}$ of 2% and an error on the unpolarised gluon density $G(x)$ of 5% [22]. We assume that the unpolarised quantities will be measured before with high statistical precision with the HERA high-luminosity upgrade. The uncertainty on the ratio of the polarised and unpolarised quark densities, $\Delta q/q$, was considered to be 10%, based on present fixed target measurements of $g_1(x)$, and the error on the polarisation measurement was taken to be 5% for each beam. These contributions were added in quadrature and the result is displayed as a shaded band in the Fig. 7a and 7d. The largest contribution is due to the uncertainty on the beam polarisations and, for the two highest x-bins, due to the QCDC contribution. Other studies, such as the influence of the choice of the fragmentation model on the result, have also been performed, but no significant change of the results could be observed. In summary we see that for all x bins the statistical uncertainty is dominating.

In Table 2 the expected statistical errors, corresponding to a luminosity of 500 pb^{-1}, are detailed for the measurable x-bins and for the first moment $\int \Delta G dx$ in the range of $0.0015 < x < 0.32$. The result we obtain is:

$$\delta\left(\int_{0.0015}^{0.32} \Delta G dx\right) = 0.21. \tag{7}$$

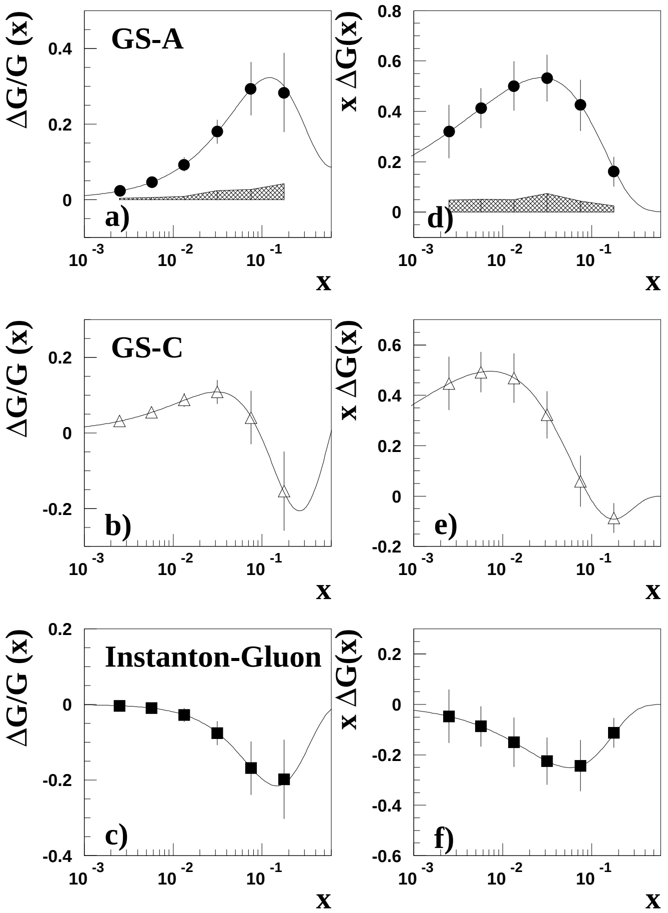

Figure 7: Sensitivity to $\Delta G/G$ (a-c) and $x\Delta G$ (d-f) for a luminosity of 500 pb^{-1}.

The table also shows an interesting combination of this result with a proposed measurement of $\Delta G/G$ from prompt photon production of jets in polarised pp-scattering, called HERA-$\vec{N}$ [23]. The idea is to scatter the polarised protons from the HERA collider on a polarised fixed proton target. The luminosity assumed for this experiment is 240 pb^{-1} corresponding to about 3 years of running in parallel with the collider experiments. Such an experiment would cover an almost completely complimentary x-range. Combining the two x-ranges leads to the result, which is shown in the last row of the table. The individual results entering into the combinations are given on top. The covered x-range is increased to $0.0015 < x < 0.5$ and the result on the error of the first moment of ΔG is:

$$\delta\left(\int_{0.0015}^{0.5} \Delta G dx\right) = 0.20. \tag{8}$$

A comparison of the accessible x-ranges for this and other proposed experiments is also shown in Fig. 8. Displayed is the expected di-jet result from polarised ep scattering at HERA (HERA 2+1 jet), the HERA-$\vec{N}$ γ+jet measurement, and the expected accuracy from a measurement of γ+jet in polarised pp collisions with the STAR detector at RHIC [24] for $Q^2 = 20$ GeV^2. The di-jet measurement at a polarised HERA clearly extends into a region of x which is not accessible to any other experiment! Also shown are four different parametrizations for the polarised gluon densities. In addition to the previously used 'gluons sets A and C' of Gehrmann and Stirling also the 'gluon set B' of the same authors and the 'standard scenario' of Glück, Reya, Stratmann and Vogelsang (GRSVs) [25] (all LO) are shown. All these parametrizations are in agreement with present data.

x	$\delta(\Delta G(x)/G(x))$	$\delta(\int \Delta G dx)$
0.0015 - 0.0036	0.007	0.082
0.0036 - 0.009	0.009	0.072
0.009 - 0.022	0.002	0.092
0.022 - 0.054	0.003	0.098
0.054 - 0.13	0.068	0.099
0.13 - 0.32	0.095	0.058
Σ 0.0015 - 0.32	0.019	0.21
Σ 0.0015 - 0.1 (di-jets)	0.006	0.20
Σ 0.1 - 0.5 (HERA-$\vec{N}$)	0.017	0.021
Σ 0.0015 - 0.5 (di-jets + HERA-$\vec{N}$)	0.018	0.20

Table 2: Expected uncertainties on $\Delta G/G$ and the first moment of $\Delta G(x)$ for the measured x-bins. The upper seven rows show errors for each x-bin and the sum over the full measured range of the di-jet analysis. In the lower three rows the di-jet measurement has been combined with a possible measurement of $\Delta G/G$ from prompt photon + jet production at HERA-$\vec{N}$.

The first moments of all the Gehrmann-Stirling sets are very similar (2.6, 2.6, and 2.5 at $Q^2 = 20$ GeV^2 for the sets A, B, C, respectively, and 1.8 for GRSVs). The shape of $\Delta G(x)$, however, can be very different, which shows the importance of this kind of measurement with respect to e.g. extractions of the first moment of ΔG in a NLO-QCD analysis of the polarised structure function g_1. However, since these two approaches give rather complementary information it could be advantageous to combine the di-jet analysis and the NLO fits to g_1 into a common fit. A case study of such an analysis for a polarised HERA has been performed [26].
Another point to stress here is that for all four parametrizations the part of the first moment $\int_{0.0015}^{0.32} \Delta G dx$ which can be measured with the di-jet events is 60% for GS-C and about 75% for GS-A, GS-B, GRSVs of the total first moment $\int_0^1 \Delta G dx$. As an example, assuming GS-A, in this experiment we would measure $\int_{0.0015}^{0.32} \Delta G dx = 2.0 \pm 0.21$(stat.), hence a 10% uncertainty for the first moment in the measured range.

To show that more information could be extracted, Fig. 9 shows the expected statistical uncertainty on $\Delta G/G$ (a,b) and $x\Delta G$ (c,d) for two bins of Q^2. A luminosity of 500 pb^{-1} and the GS-A polarised gluon distribution are assumed. The data were divided as given in Table 1. It shows that such analysis can provide direct information on the interesting question on the Q^2 dependence of ΔG.

5 Conclusions

We have shown in this study that an analysis of the di-jet rate at HERA allows a measurement of $\Delta G/G(x)$ in an x-range from $0.002 < x < 0.2$, a region where large differences are observed between present models for the polarised gluon distribution. This x range is largely uncovered by any other proposed experiment. The precision of the measurement, both statistical and systematical, is large enough such that shape of $\Delta G/G$ could be measured and discrimination between different polarised gluon distributions would be possible. The first moment of ΔG can be determined with a precision of about 10%, in the range $0.0015 < x < 0.32$. The results are

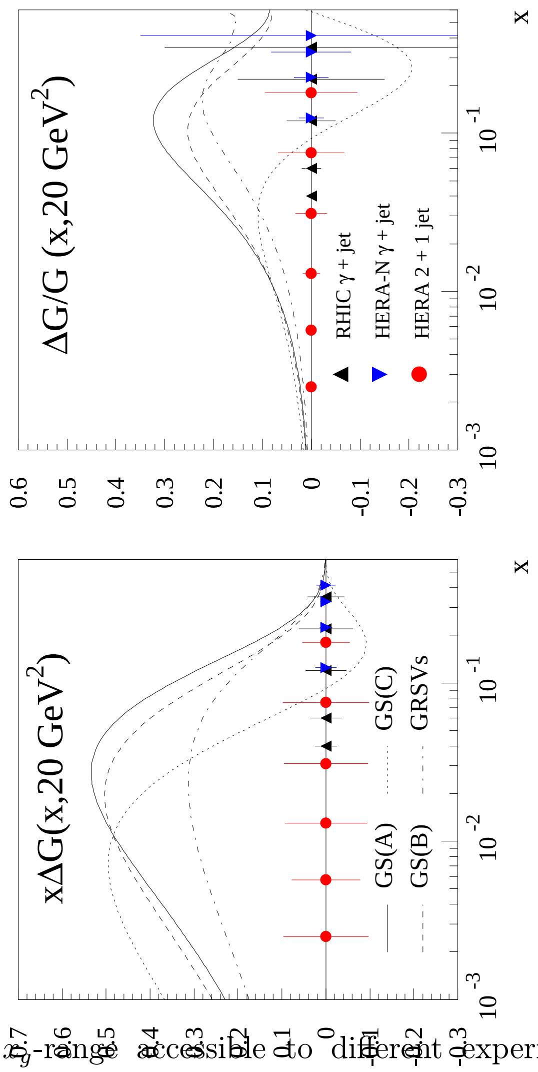

Figure 8: The x_g-range accessible to different experiments for measuring ΔG. Different parametrizations of the polarised gluon density are shown as well, to demonstrate the separation power of the measurements.

r]

complimentary to extractions of the first moment of ΔG from structure function measurements, and measurements at COMPASS [27], RHIC or HERA-$\vec{N}$. The proposed measurement is vital for our understanding of the spin structure of the nucleon.

Acknowledgments

We thank T. Gehrmann, F. Kunne and E. Mirkes for helpful discussions.

References

[1] EMC, J. Ashman et al., *Phys. Lett.* **B206** (1988) 364; and *Nucl. Phys.* **B328** (1989) 1.

[2] H1 Collab., S. Aid et al., *Nucl. Phys.* **B445** (1995) 3.

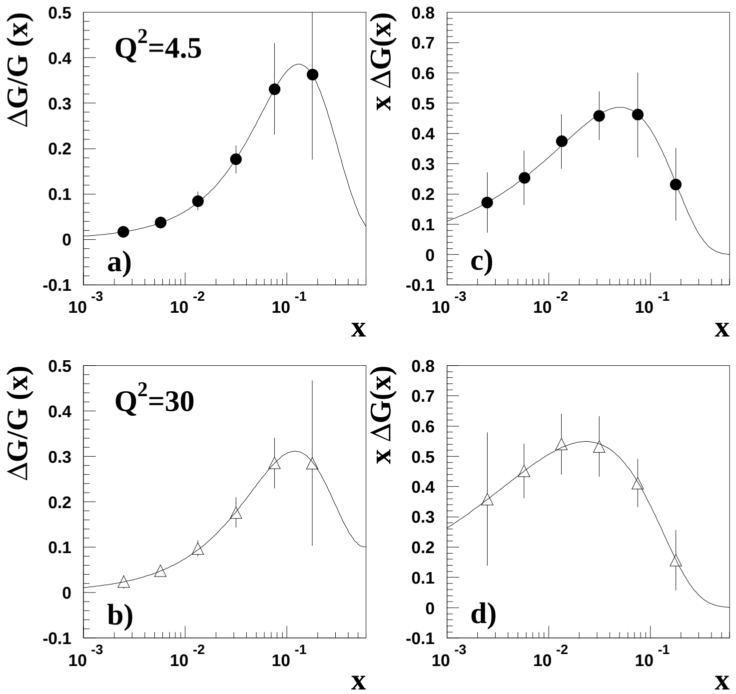

Figure 9: Sensitivity to $\Delta G/G$ (a,b) and $x\Delta G$ (c,d) when splitting the data into two bins of Q^2. The low-Q^2 cut was reduced to $Q^2 > 2$ GeV^2. The assumed luminosity is 500 pb^{-1}.

[3] H1 Collab., contributed paper to ICHEP97, Jerusalem (1997), `ICHEP97-275`.

[4] J. Repond, proceedings of workshop 'Deep Inelastic Scattering and Related Phenomena', Rome 1996, Eds. G. D'Agostini and A. Nigro (World Scientific, Singapore, 1997) 439.

[5] D.P. Barber et al., proceedings of workshop 'Future Physics at HERA', Eds. G. Ingelman, A. De Roeck, R. Klanner, DESY (1996) 1205.

[6] J. Feltesse, F. Kunne, E. Mirkes, *Phys. Lett.* **B388** (1996) 832.

[7] A. De Roeck et al., `hep-ph/9610315` and proceedings of workshop 'Future physics at HERA', Eds. G. Ingelman, A. De Roeck, R. Klanner, DESY (1996) 803.

[8] T. Gehrmann, W.J. Stirling, *Phys. Rev.* **D53** (1996) 6100.

[9] N. Kochelev, `hep-ph/9707418`, and these proceedings.

[10] T. Schäfer, E.V. Shuryak, `hep/ph9610451` (1996);
D.I. Diakonov, `hep-ph/9602375` (1996).

[11] M. Glück, E. Reya, A. Vogt, *Z. Phys.* **C67** (1995) 433.

[12] E. Mirkes, D. Zeppenfeld , *Phys. Lett.* **B380** (1996) 205.

[13] E. Mirkes et al., these proccedings.

[14] L. Mankiewicz, A. Schäfer, M. Veltri, *Comp. Phys. Comm.* **71** (1992) 305.

[15] O. Martin, M. Maul and A. Schäfer, `hep/ph-971038` and these proceedings.

[16] G. Ingelman, A. Edin, J. Rathsman, *Comp. Phys. Comm.* **101** (1997) 108.

[17] M. Maul et al., `hep-ph/9710309`

[18] G. Ingelman, A. Edin, J. Rathsman, *Z. Phys.* **C75** (1997) 57.

[19] M. Wobisch, to appear in the proceedings of the workshop 'DIS and Related Topics', Chicago 1997, Eds. D. Krakower and J. Repond.

[20] T. Sjöstrand, *Comp. Phys. Comm.* **82** (1994) 74.

[21] G. Contreras, these proceedings.

[22] M. Botje, M. Klein, C. Pascaud, proceedings of workshop 'Future physics at HERA', Eds. G. Ingelman, A. De Roeck, R. Klanner, DESY (1996) 33.

[23] M. Anselmino et al., proceedings of workshop 'Future physics at HERA', Eds. G. Ingelman, A. De Roeck, R. Klanner, DESY (1996) 837, and these proceedings.

[24] S. Heppelmann, proceedings of '12th Int. Symposium on High Energy Spin Physics', Amsterdam 1996, Eds. C.W. de Jager et al. (World Scientific, Singapore, 1997) 352.

[25] M. Glück, E. Reya, M. Stratmann, W. Vogelsang, *Phys. Rev.* **D53** (1996) 4775.

[26] A. Deshpande et al., these proceedings

[27] COMPASS proposal, `CERN/SPSLC/P297`.

"These Proceedings" refers to the Proceedings of the Workshop on Physics at HERA with Polarized Protons and Electrons.

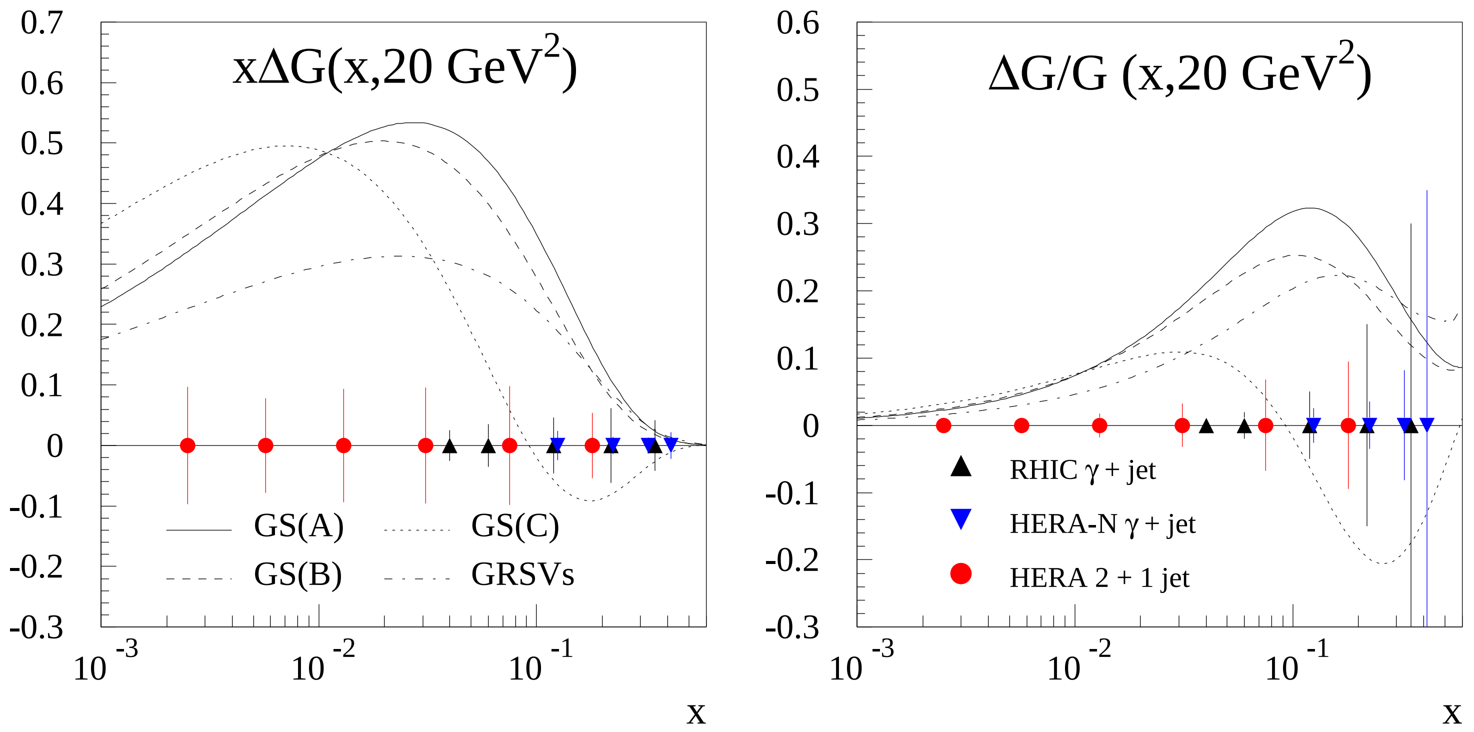

xΔG(x,20 GeV²)
GS(A)
GS(C)
GS(B)
GRSVs
ΔG/G (x,20 GeV²)
RHIC γ + jet
HERA-N γ + jet
HERA 2 + 1 jet
x

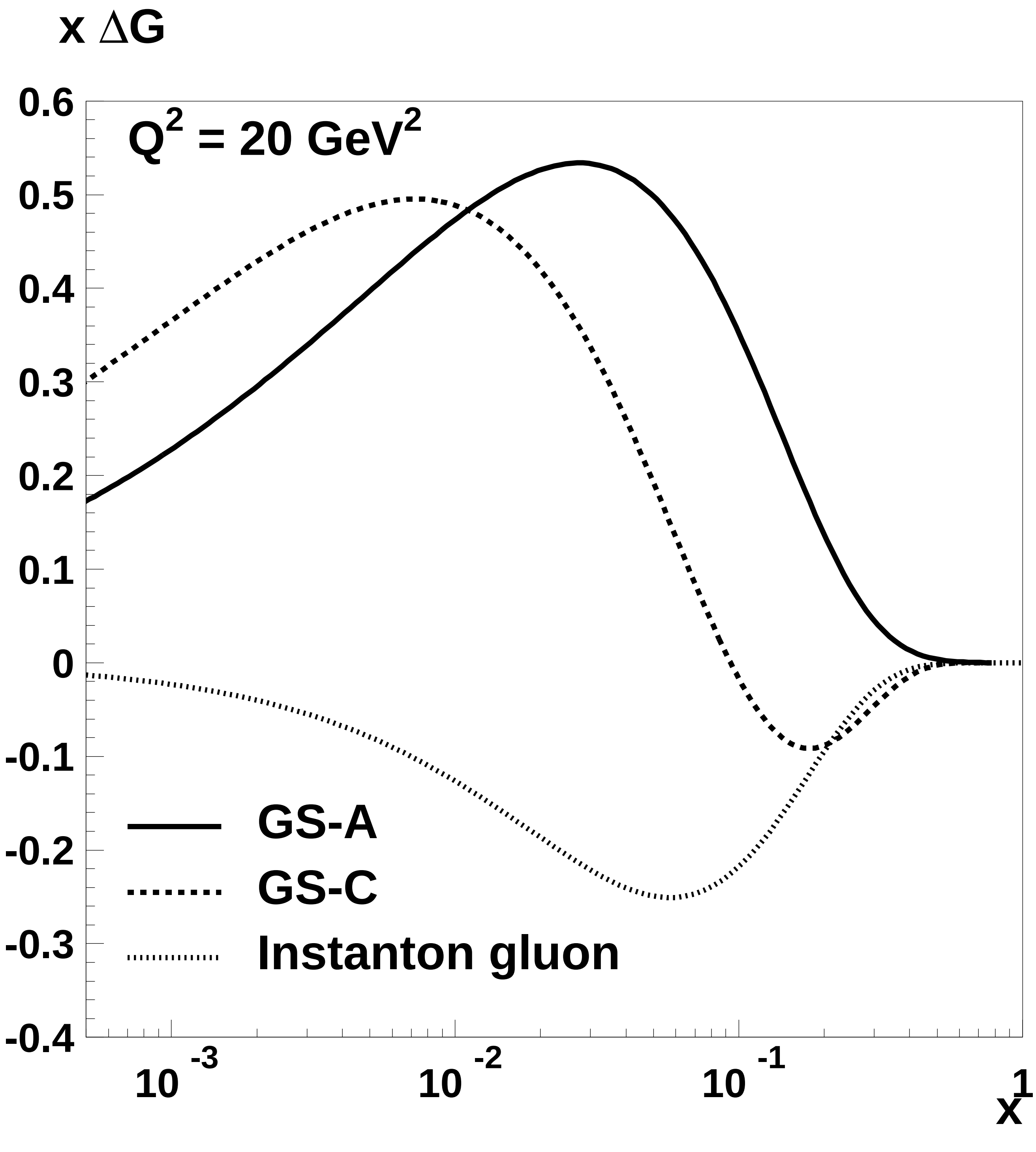
x ΔG
Q^2 = 20 GeV^2
0.6
0.5
0.4
0.3
0.2
0.1
0
-0.1
-0.2
-0.3
-0.4
GS-A
GS-C
Instanton gluon
10^-3
10^-2
10^-1
1
x

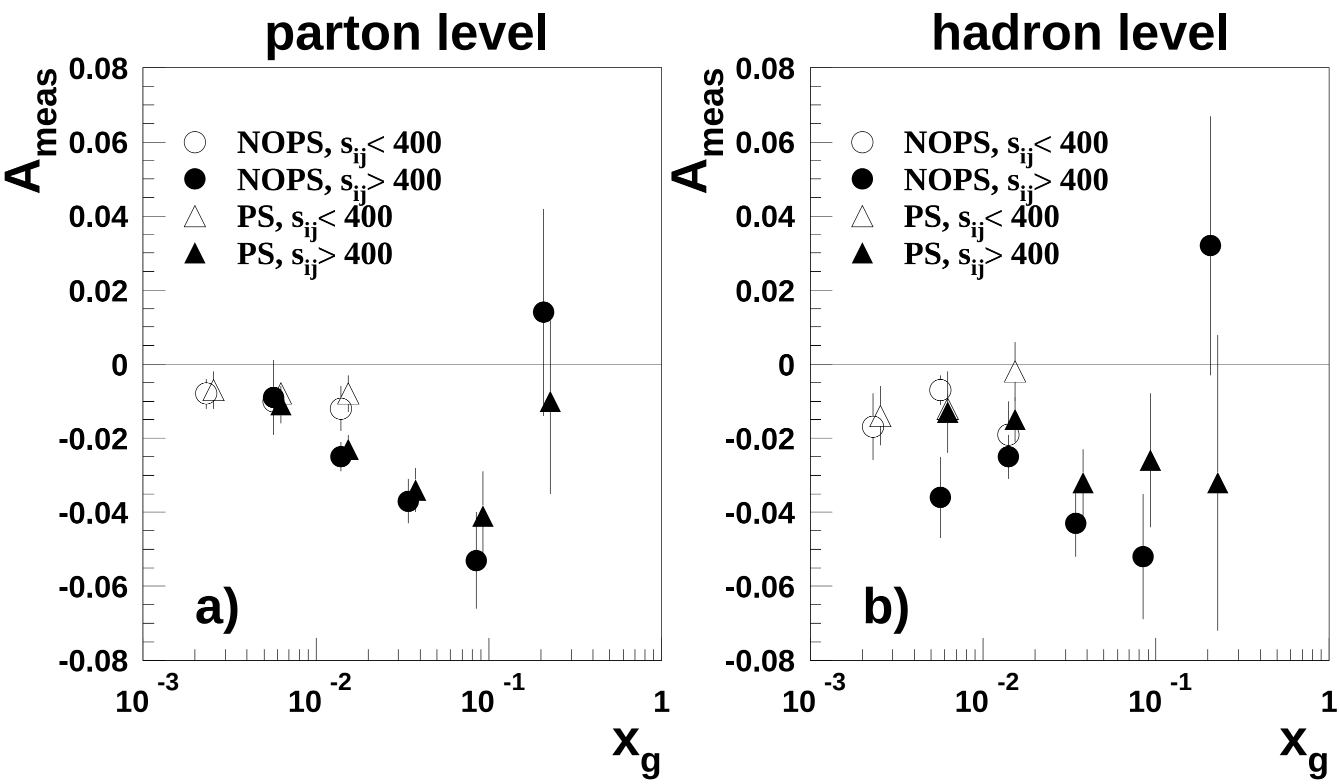
parton level
hadron level
A_meas
0.08
0.06
0.04
0.02
0
-0.02
-0.04
-0.06
-0.08
NOPS, s_ij< 400
NOPS, s_ij> 400
PS, s_ij< 400
PS, s_ij> 400
a)
b)
10 -3
10 -2
10 -1
1
x_g

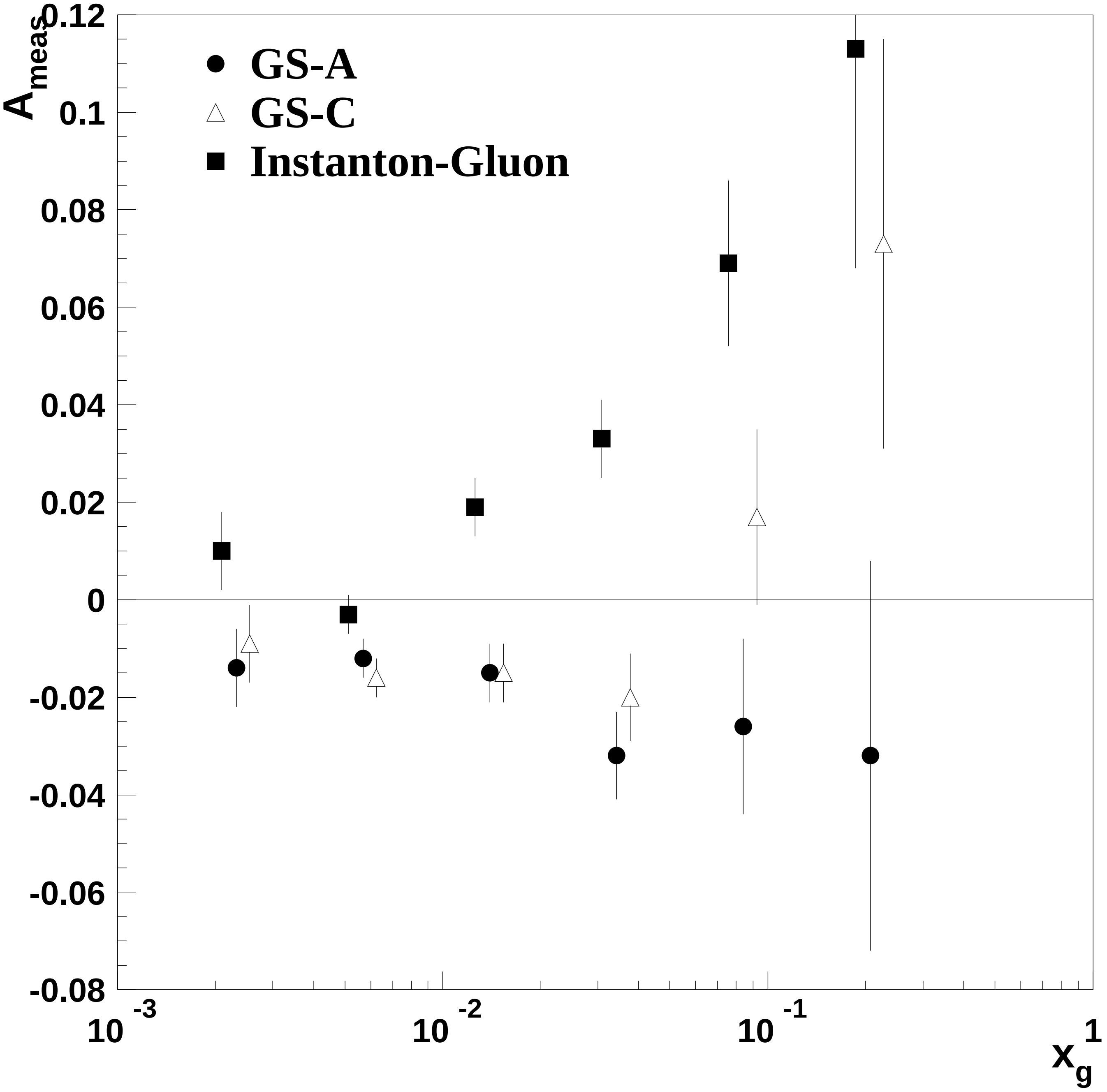

A_meas
GS-A
GS-C
Instanton-Gluon
0.12
0.1
0.08
0.06
0.04
0.02
0
-0.02
-0.04
-0.06
-0.08
10 -3
10 -2
10 -1
1
x_g

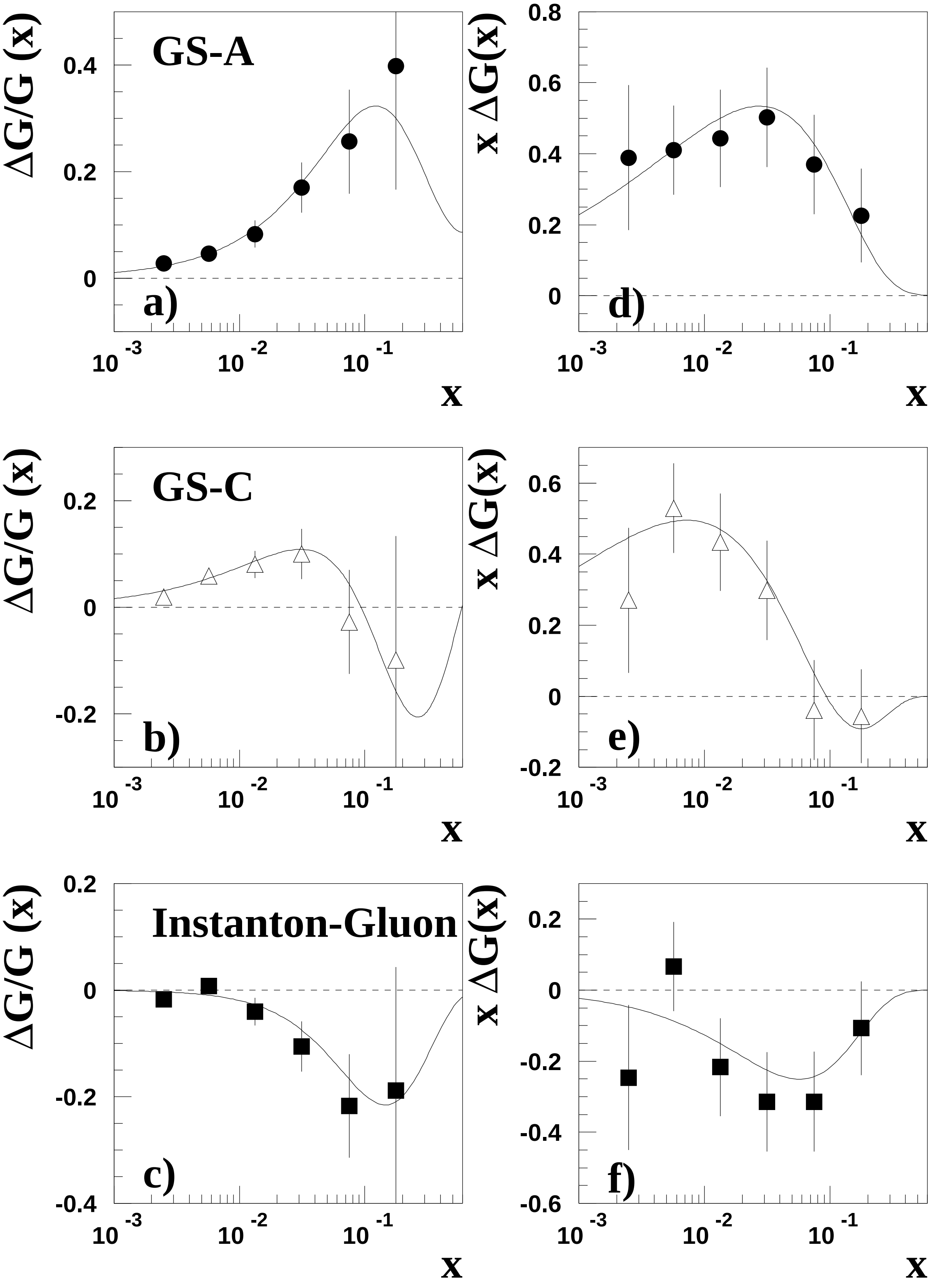

GS-A
GS-C
Instanton-Gluon
ΔG/G (x)
x ΔG(x)
a)
b)
c)
d)
e)
f)
x

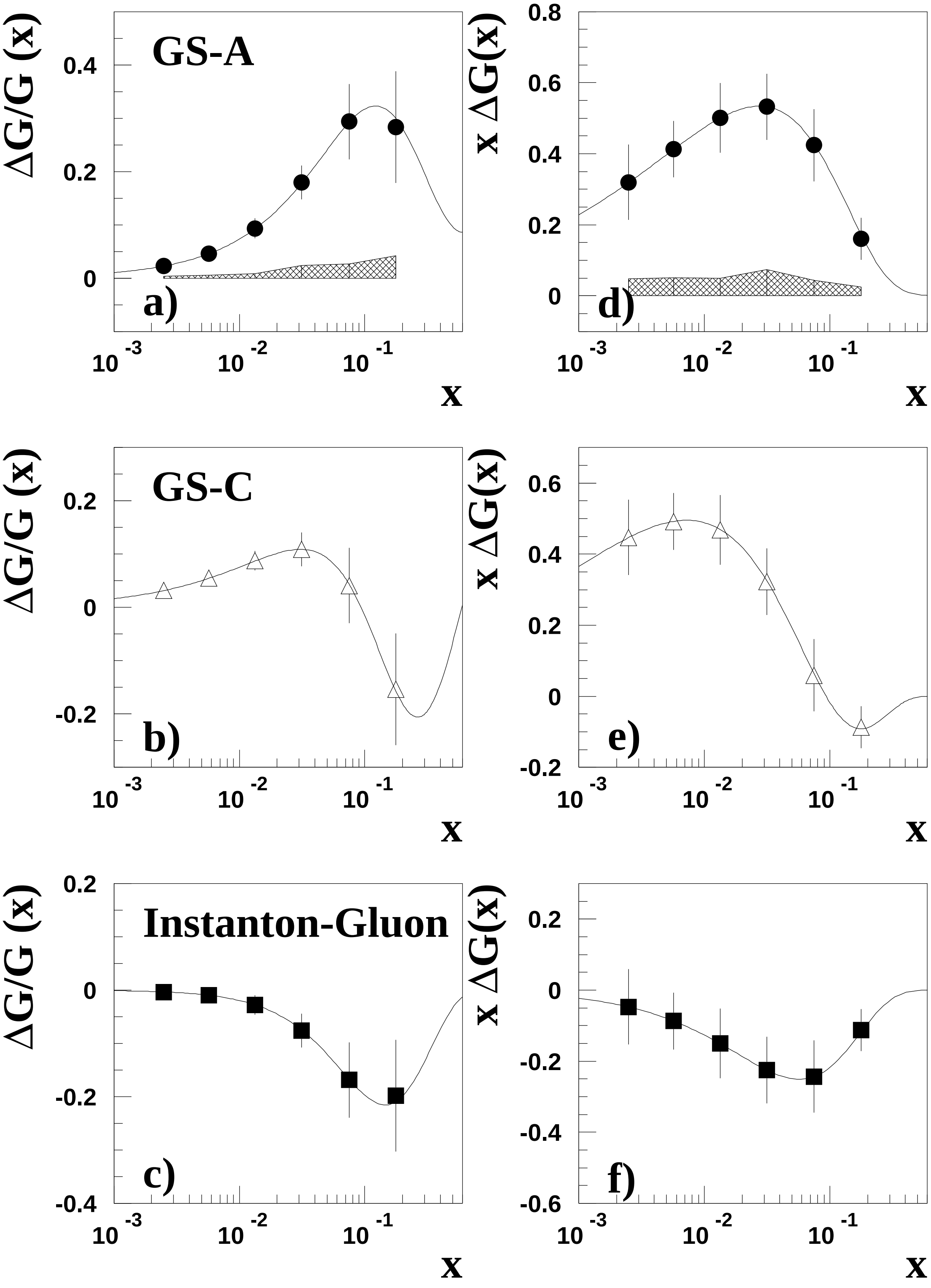
GS-A
GS-C
Instanton-Gluon
ΔG/G (x)
x ΔG(x)
a)
b)
c)
d)
e)
f)
x
0.4
0.2
0
-0.2
-0.4
0.8
0.6
-0.6
10 -3
10 -2
10 -1

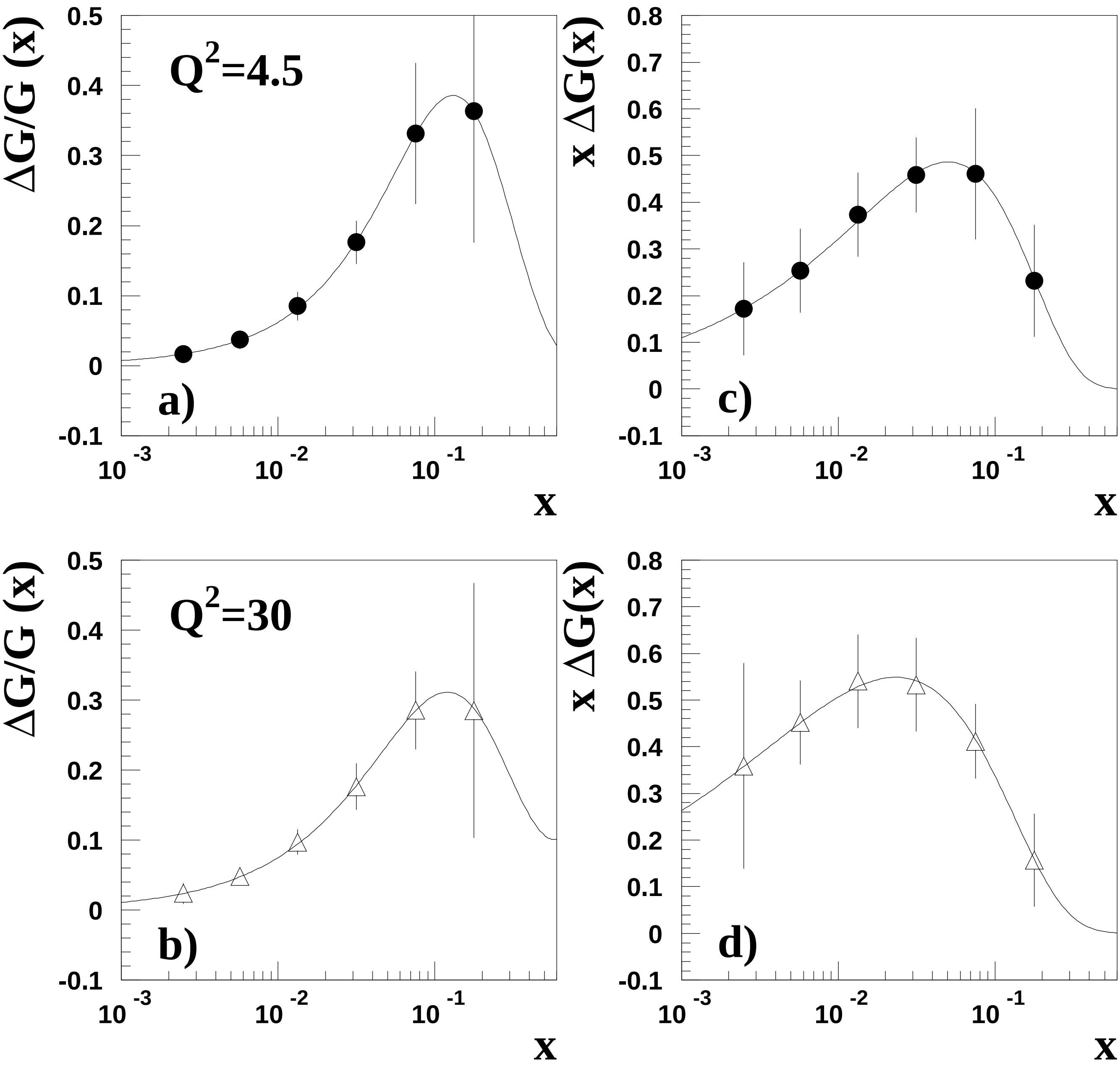

ΔG/G (x)
Q^2=4.5
a)
x
ΔG/G (x)
Q^2=30
b)
x
x ΔG(x)
c)
x
x ΔG(x)
d)
x